Preliminary Analysis and Member Sizing of Tall Tubular Steel Buildings

CHOW H. WONG, MAHJOUB M. EL NIMEIRI AND JOHN W. TANG

More and more tall, slender multistory buildings have been designed and built in the last decade. For steel buildings in particular, the present architectural trend is toward the use of light panels with large glass areas. This trend requires the structural steel tube not only to resist all lateral loads to limit the drift to some acceptable values, but also to prevent racking of the glass panels.

The analysis of tall steel tubes to account for all the lateral loads has been well established in the literature.[1,2,6,8]

Most available commercial computer programs, such as SAPIV, STRUDL II, NASTRAN, etc., are equipped to perform analysis of such systems both accurately and efficiently, but they are costly and time consuming. Therefore, the tendency is to limit their use for the so-called final analysis only.

One of the major problems remaining is how to conduct an efficient and accurate preliminary analysis and select almost optimum member sizes to be used in the final computer analysis. Considerable work has been devoted to this problem.[4,5,7]

The important factors affecting the behavior of the tube are height-to-width ratio (the higher the ratio the more effective is the tube action), bay width, story height, setbacks, shape and geometry of system, etc. Narrow bays are understood to give a better tube behavior. However, shear deformation of short beams reduces their bending efficiency, a fact which has been overlooked. The interaction of frame action, cantilever behavior and warping effects, although identified, has not been closely investigated.

Chow H. Wong is Project Engineer, Skidmore, Owings & Merrill, Chicago, Illinois.

Mahjoub M. El Nimeiri is Associate, Skidmore, Owings & Merrill, Chicago, Illinois.

John W. Tang is Structural Analyst, UCS, Minneapolis, Minnesota.

This paper addresses itself to two problems. First, it presents a consistent and highly accurate approach for the analysis and for member proportioning of two- or three-dimensional, rectangular (but symmetrical), tubular steel multistory frames subjected to gravity and lateral loads. The analysis as written here means the calculations of lateral displacements and member forces. The analysis is based on the assumption that the system is made up of two linearly independent systems, a frame and a cantilever, superimposed over each other (see Fig. 1). The calculations of the frame were based on the slope deflection method, neglecting axial strains, but including shear deformations and assuming that all points of contraflexure occur at member midspans.

The cantilever is assumed to be slender (i.e., no shear deformation) and is made up of the columns which resist loads by their axial stiffness only. The members used in this analysis are either W shapes or built-up I-sections. The

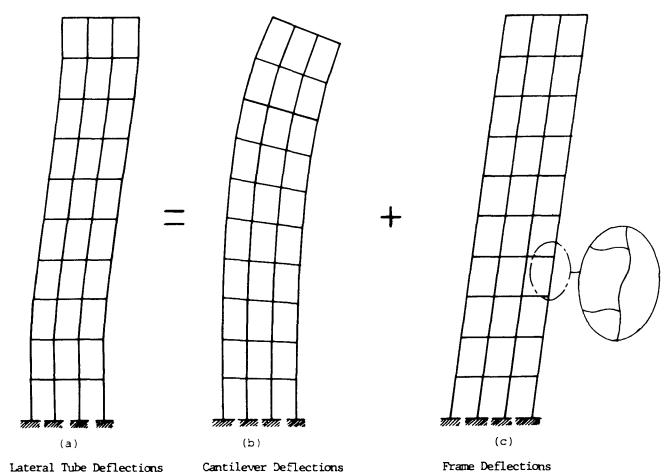

Figure 1

analysis is accurate within the limitations of the assumptions made.

Second, the paper presents a complete study of the effect of shear deformations on the stiffness of beams and columns and, hence, the overall stiffness of the tube. The shear stiffness proved to be the most important factor in proportioning the spandrel beams. The paper also provides a set of design and analysis charts which could be of a great value for preliminary member sizing.

ANALYSIS

Deflection Calculations—The lateral deflection of the tube at any floor i is given by:

$$\Delta_{ti} = \Delta_{ci} + \Delta_{fi} \tag{1}$$

and

$$\Delta_{fi} = \Delta_{bi} + \Delta_{shi} \tag{2}$$

in which

Δ_{ti} = total lateral deflection at floor i
Δ_{ci} = cantilever lateral deflection at floor i
Δ_{fi} = frame lateral deflection at floor i
Δ_{bi} = bent lateral deflection at floor i
Δ_{shi} = lateral deflection due to shear leak at floor i

Frame Deflections—The basic assumptions used in the analysis are that, at any floor, (1) shear force is constant and (2) bending moment diagrams are such that contraflexure points occur at midspan of both girders and columns. Consider Fig. 2. By using the slope deflection method or any other similar method, the bent lateral displacement Δ_{bi}, which is the relative displacement between end A and end B, is readily given by:

$$\Delta_{bi} = \frac{VH_i^2}{12E}\left(\frac{1}{2K_{gi}} + \frac{1}{2K_{ci}}\right) \tag{3}$$

where

$K_{gi} = I_{gi}/L_{gi}$
$K_{ci} = I_{ci}/H_i$
H_i = the story height

and for all the bents in level i,

$$\Delta_{bi} = \frac{VH_i^2}{12E}\left(\frac{1}{\Sigma K_{gi}} + \frac{1}{\Sigma K_{ci}}\right) \tag{4}$$

This is essentially similar to the equation developed by Manney-Goldberg.[3]

Now consider Fig. 3, which shows the lateral deflections of a deep beam due to shear only. The rotation at the center is given by:

$$\frac{d\,(\Delta_{sh})}{d\,x} = \frac{V}{A'_g\,G} \tag{5}$$

where A' is the effective shear area, and G is the modulus of shear rigidity. Integrating Eq. (5) yields:

$$\Delta_{sh} = \frac{VL}{A'_g\,G} \tag{6}$$

which is the deflection of a beam of length L due to shear leak under constant shear force V. Applying Eq. (6) to the bent in Fig. 2, the following equation is readily given:

$$\Delta_{shi} = \frac{VH_i^2}{G}\left(\frac{1}{\Sigma A'_{gi}L_{gi}} + \frac{1}{\Sigma A'_{ci}H_i}\right) \tag{7}$$

where

A'_{gi} is the effective shear area of girder at level i
A'_{ci} is the effective shear area of column at level i

Hence, Eq. (2) can be rewritten as:

$$\Delta_{fi} = \frac{VH_i^2}{12E}\left[\frac{1}{\Sigma K_{ci}}(1 + C_c) + \frac{1}{\Sigma K_{gi}}(1 + C_g)\right] \tag{8}$$

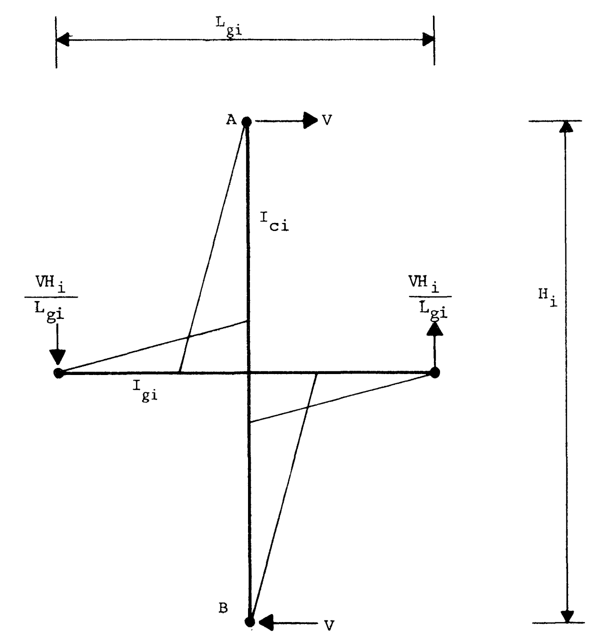

Fig. 2. Typical interior bent forces

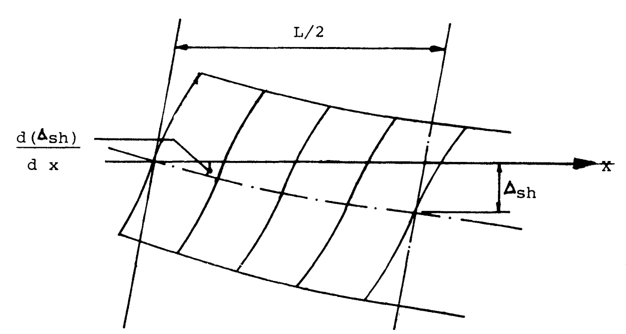

Fig. 3. Lateral shear deformation in a deep beam

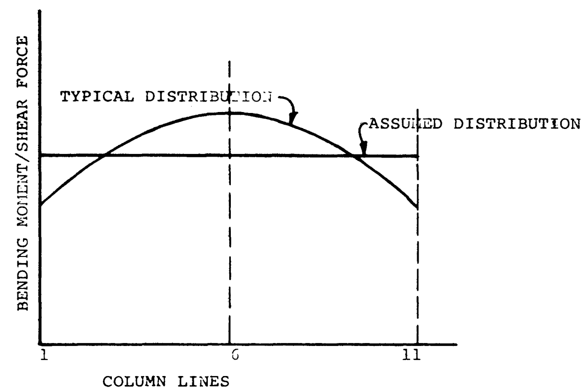

Fig. 4. Exact vs. assumed distribution of bending moments and shear forces

and for Poisson's ratio $\nu = 0.25$,

$$C_c = 30 \times \frac{I_{ci}}{A'_{ci} H_i^2}$$

$$C_g = 30 \times \frac{I_g}{A'_{gi} L_{gi}^2}$$

Cantilever Deflections—Cantilever deflections can be calculated readily using the moment area method. The moment of inertia, I_o, of the cantilever is variable along the height of the structure, but at any level i, $I_{oi} = \Sigma A_{ci} r^2_i$, where I_{oi} is the moment of inertia of the cantilever at level i, A_{ci} is the column area at level i, and r_i is the distance of the column from the centroid of the cantilever.

Force Calculations—After the prescribed drift ratios are satisfied and all the stiffness requirements are met, a member force check is conducted.

The forces of the system are calculated based on the same deflection models and no additional assumptions are made:

1. The cantilever analysis gives the axial forces on the column only and they vary linearly across the floor.
2. The frame analysis gives the bending moments and shear forces for both the beams and columns (see Fig. 2). These forces are essentially average values, although the sum of these forces at any level i satisfies equilibrium. There is a slight redistribution (see Fig. 4).
3. This force analysis ignores the effect of shear lag and the relative upward movement between the beams and columns. However, for all practical purposes, the results are adequate, as can be seen from the examples presented later in this paper.

Shear Leak Effect—The effect of shear deformations on the stiffness of the spandrel beam or column is termed here as the "shear leak effect."

Spandrel Beam—Shear leak term from Eq. (8):

$$C_g = 30 \times \frac{I_{gi}}{A'_{gi} L_{gi}^2}$$

For a built-up I-section, both I_{gi} and A'_{gi} are constant and dependent.

For a fixed cross section, $C_c \rightarrow 0$ when $L_{gi} \rightarrow \infty$; hence, no reduction in stiffness due to shear. On the other hand, when $L_{gi} \rightarrow 0$, the shear leak term blows up and the structure's lateral deflections $\rightarrow \infty$.

If L_g is kept constant and the ratio of A'_{gi} to A is varied from 0.3 to 0.5, the shear leak term exhibits a gentle slope and stays almost horizontal, indicating that is the optimum range.

NUMERICAL EXAMPLES

The following examples examine the behavior of the frame-tube building, using the method outlined previously. The results are then compared with the exact analysis performed by the computer program, SAP-IV. For preliminary analysis purposes, the contribution of the "flange-frame" in resisting the lateral loading can be approximated by the method outlined in Ref. 7. The effect of the flange-frame is considered in Example 2.

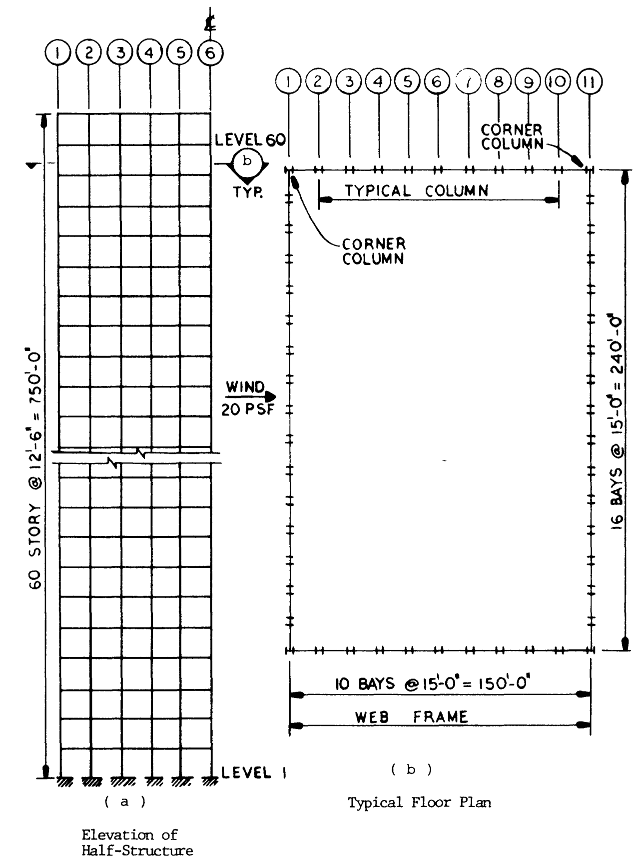

Figure 5

Table 1. Section Properties for Example 1

Level	Beam	Typical Column	Corner Column
60–56	W30X116	W30X99	W30X99
55–51	W36X135	W30X116	W36X135
50–46	W36X135	W36X135	W36X182
45–41	W36X182	W36X160	W36X260
40–36	W36X230	W36X194	W36X280
35–31	W36X260	W36X230	BU24 × 42 ($t_f = 1\frac{1}{2}, t_w = 1$)
30–26	W36X300	W36X260	BU24 × 42 ($t_f = 1\frac{3}{4}, t_w = 1\frac{1}{4}$)
25–21	W36X300	W36X300	BU24 × 42 × $2\frac{1}{4}$
20–16	BU16 × 42 ($t_f = 2\frac{1}{2}, t_w = 1\frac{1}{2}$)	BU16 × 42 ($t_f = 2\frac{1}{2}, t_w = 1\frac{1}{2}$)	BU24 × 42 ($t_f = 2\frac{3}{4}, t_w = 1\frac{1}{2}$)
15–11	BU16 × 42 ($t_f = 2\frac{1}{2}, t_w = 1\frac{1}{2}$)	BU16 × 42 ($t_f = 2\frac{1}{2}, t_w = 1\frac{1}{2}$)	BU24 × 42 ($t_f = 3, t_w = 1\frac{3}{4}$)
10–6	BU16 × 42 ($t_f = 3\frac{1}{2}, t_w = 1\frac{3}{4}$)	BU16 × 42 ($t_f = 3\frac{1}{4}, t_w = 1\frac{3}{4}$)	BU24 × 42 ($t_f = 3\frac{1}{2}, t_w = 2$)
5–1	BU16 × 42 ($t_f = 3\frac{1}{2}, t_w = 1\frac{3}{4}$)	BU16 × 42 ($t_f = 3\frac{1}{2}, t_w = 1\frac{3}{4}$)	BU24 × 42 ($t_f = 3\frac{1}{2}, t_w = 2$)

Note: BU indicates built-up section.

Example 1—A 60-story steel frame-tube building with a height-to-width ratio of 5.0 is considered. The building geometry is shown in Fig. 5. The building is considered fixed at the base and is analyzed for a lateral load of 20 psf on the long face of the building. Lateral resistance is considered to be offered by the two "web-frames" only. A preliminary sizing of the columns is obtained from gravity consideration; with these sizes, the deflection due to the cantilever action is calculated using the moment-area or another similar method. In this case, the tip deflection is found to be 10.3 in. In order to limit the total building drift to within $H/500$ = 18.0 in., the required stiffness of the spandrel beams is then calculated from Eq. (1). These properties are listed in Table 1. A computer analysis is then

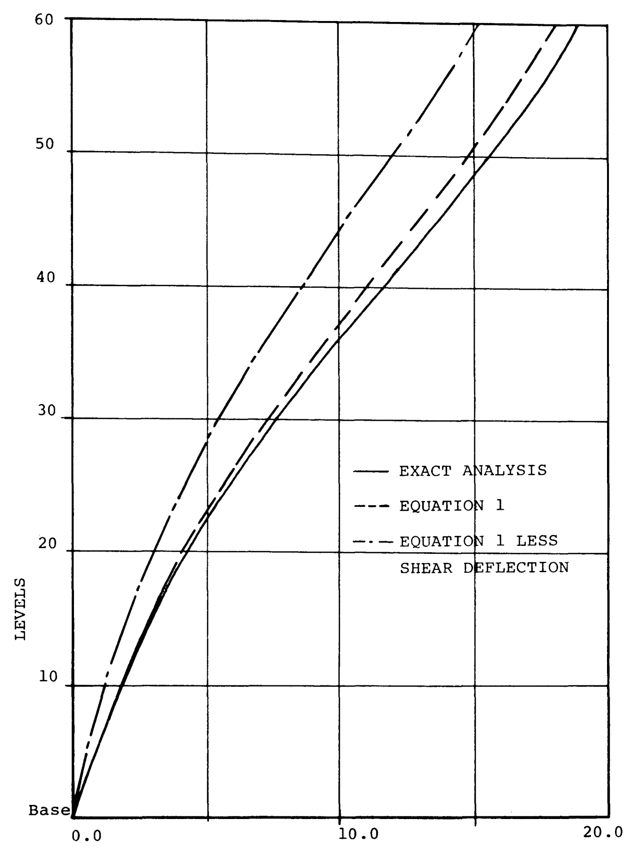

Fig. 6. Comparison of deflections (Example 1)

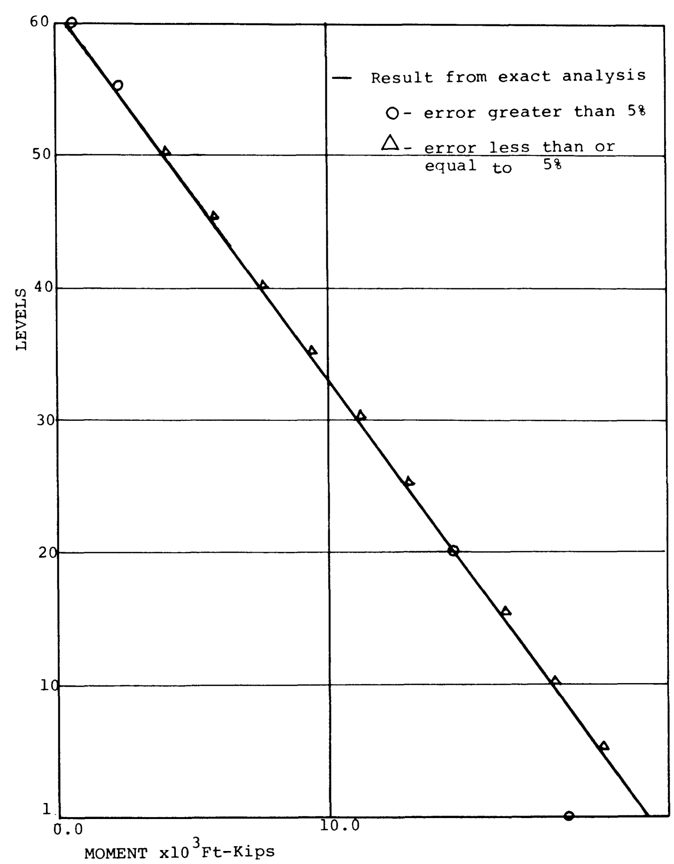

Fig. 7. Comparison of bending moments in beam/column (Example 1)

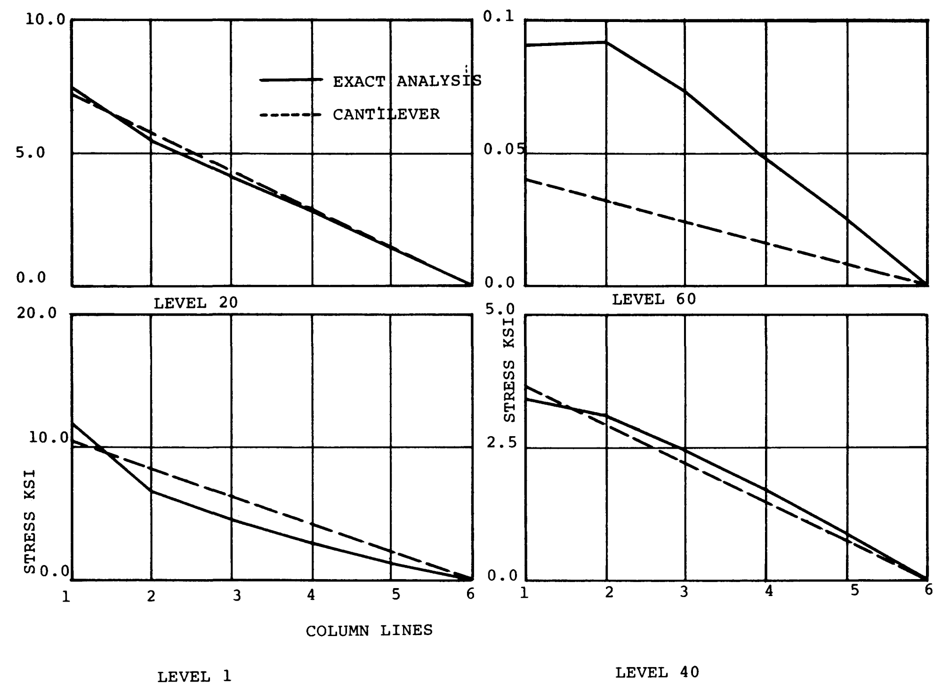

Fig. 8. Comparison of column axial forces (Example 1)

performed with this set of properties. A comparison of the deflection results is plotted in Fig. 6. The components of deflection from Eq. (1) are summarized as follows:

Cantilever deflection (Δ_c) = 10.3 in.
Bending deflection (Δ_b) = 4.9 in.
Shear leak deflection (Δ_{sh}) = 2.9 in.

The total deflection, as calculated from Eq. (1) is 18.1 in. It can be seen that cantilever deflection accounts for 57% of the total deflection. The deflection from the exact analysis is found to be 19.1 in. Hence, Eq. (1) gives an accuracy of 95% of the exact analysis. The summation of the column/beam moments at every five floor levels from the exact analysis as obtained from the method is plotted in Fig. 7.

The results compare favorably within 5% of the exact analysis, except at the first and the topmost five stories, which gives an accuracy of approximately 85% of the exact analysis.

Figure 8 shows a comparison of the column axial stresses with the results from the exact analysis. A large discrepancy can be seen in the first level and the topmost level.

Example 2—A frame-tube steel building with the same building geometry as Example 1 is analyzed. The major difference is the height of the building, which in this case, is only 24 stories high, giving a height-to-width ratio of 2.0. An average wind load of 200 kips is applied at every level. The effect of the flange-frame is considered in this case; two columns in the flange-frame are added to the corner column when computing the deflection due to column axial de-

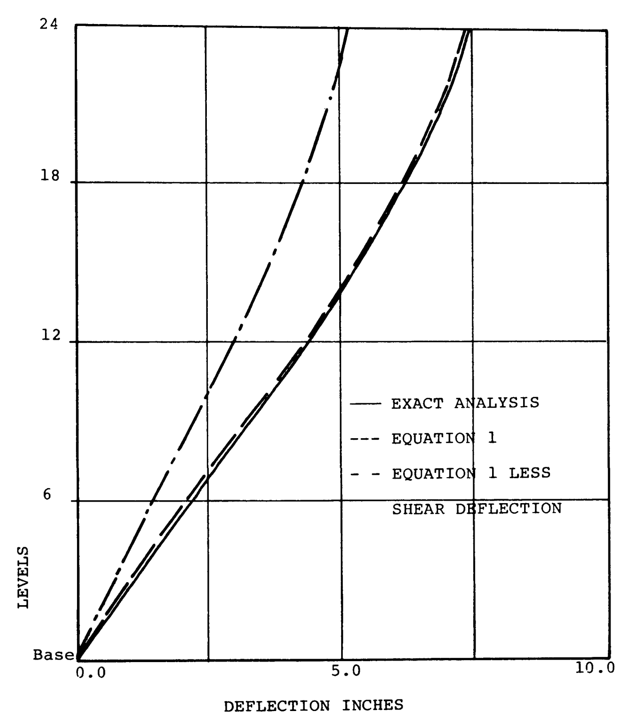

Fig. 9. Comparison of deflections (Example 2)

37

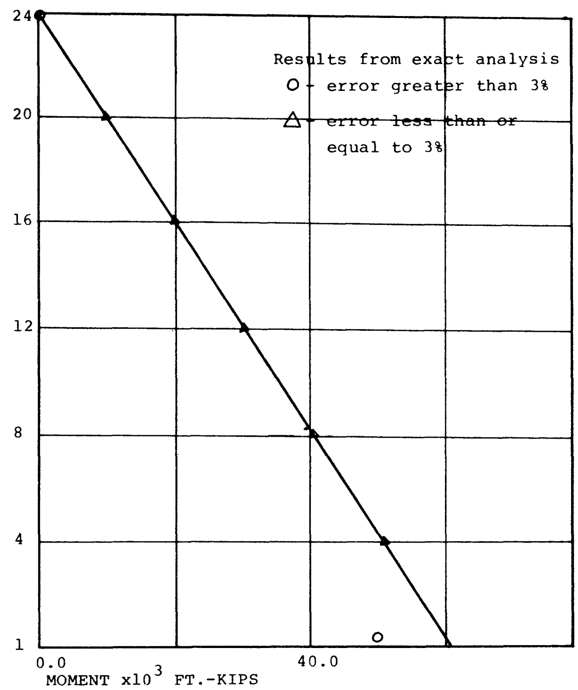

Fig. 10. Comparison of bending moments in beam/column (Example 2)

formation. In addition, beams and columns consist of only W36 sections. The result of deflection from Eq. (1) is as follows:

Cantilever deflection = 1.0 in.
Bending deflection = 4.2 in.
Shear leak deflection = 2.3 in.
Total deflection = 7.4 in.

Cantilever deflection in this case accounts for 14% of the total deflection. The results from the exact analysis show a deflection of 7.5 in. (see Fig. 9).

Similar comparisons are made for the bending moments in the beam and column. The results are plotted in Fig. 10. A comparison of the column axial stresses is shown in Fig. 11.

DESIGN AID FOR MEMBER SELECTION

Due to the relatively thin web area of an I-section, the effect of shear deformation greatly reduces its ability to control lateral deflection in a frame-tube structure. Equation (8) can be rewritten as:

$$\Delta_{fi} = \frac{VH_i}{12E}\left(\frac{1}{\Sigma \frac{I_{eff,c}}{H_i}} + \frac{1}{\Sigma \frac{I_{eff,g}}{L_{gi}}}\right) \tag{9}$$

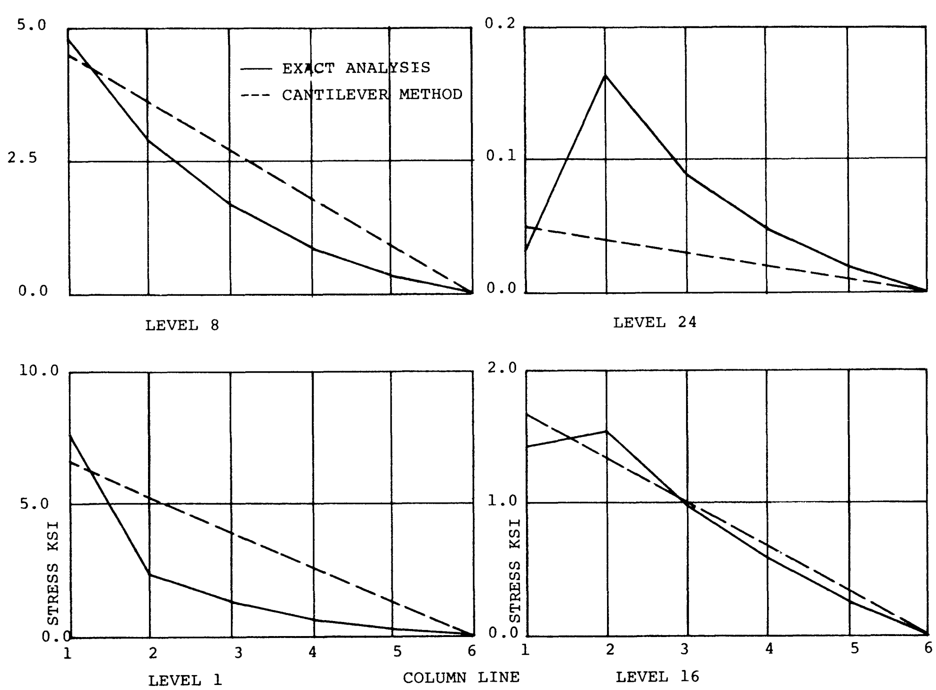

Fig. 11. Comparison of column axial stresses (Example 2)

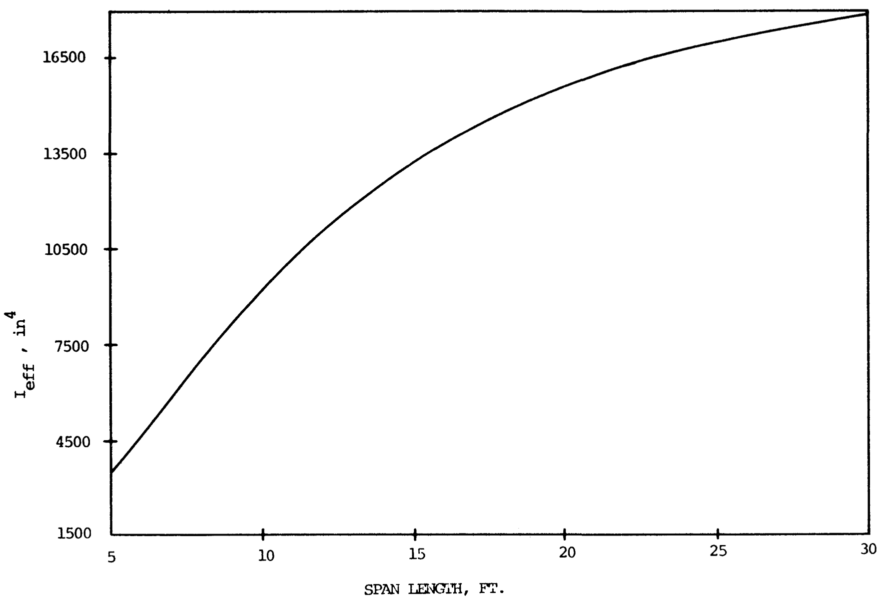

Fig. 12. Effective moment of inertia (W36x300)

where

$$I_{eff,c} = I_c/(1 + C_c)$$
$$I_{eff,g} = I_g/(1 + C_g)$$

The term I_{eff}, effective moment of inertia, can be considered as the equivalent moment of inertia of a member when bending and shear deformation subjected to lateral loading are both considered. The variation of I_{eff} of a W36x300 with respect to its length is shown in Fig. 12. It can be seen from the curve that with a member length of 10 ft, I_{eff} = 9,152 in.[4], which is only 45% of its moment of inertia. However, when the member length is increased to 30 ft, then I_{eff} = 17,900 in.[4], which is 88% of its moment of inertia. In a frame-tube steel structure, its member lengths, beam spans and column heights usually vary from 10 ft to 20 ft. It is apparent from the above illustration that the effect of shear

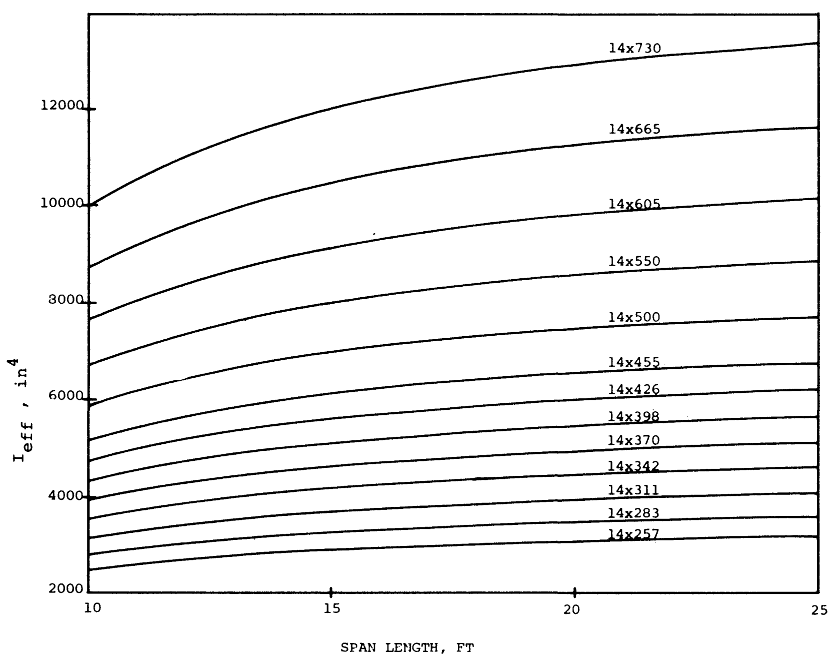

Fig. 13. Effective moment of inertia (W14x730 to W14x257)

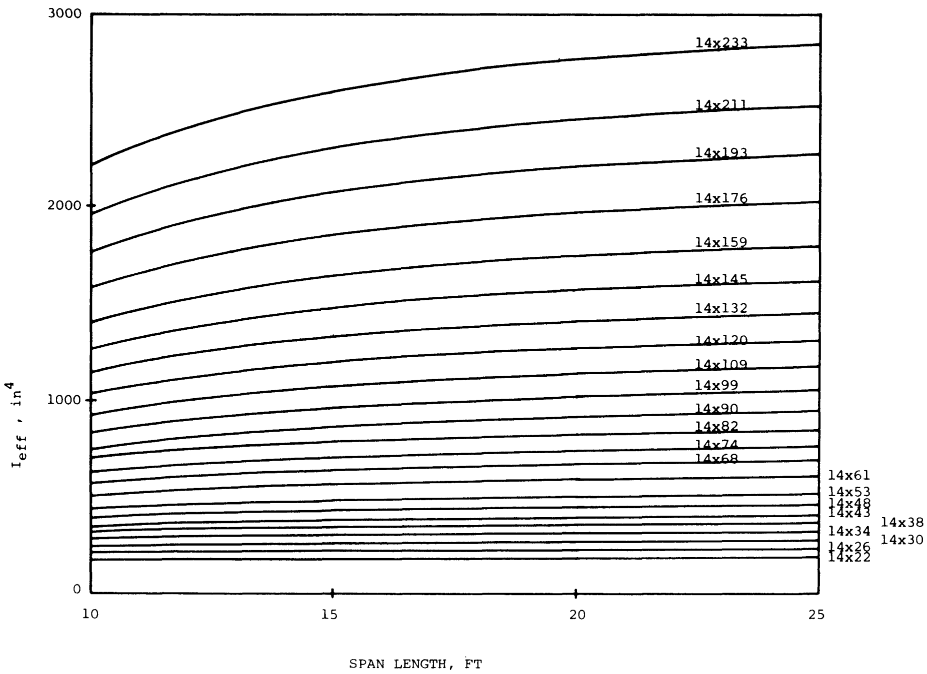

Fig. 14. Effective moment of inertia (W14x233 to W14x22)

deformation has a significant influence on the bending stiffness of an I-section. In order to assist a designer in selecting an adequate section for stiffness, the effective moments of inertias for the most frequently used sections—W14, W27, W30, W33 and W36—for member lengths between 10 ft and 25 ft, are plotted in Figs. 13 through 18.

Apart from the readily available rolled W shapes, one has to resort to built-up I-shapes for additional strength or stiffness. Consider such a shape for deflection stiffness purposes. The objective here is to optimize the section to yield the maximum effective moment of inertia. The principal parameters which affect the solution are the width and depth of the section. If architectural or other physical

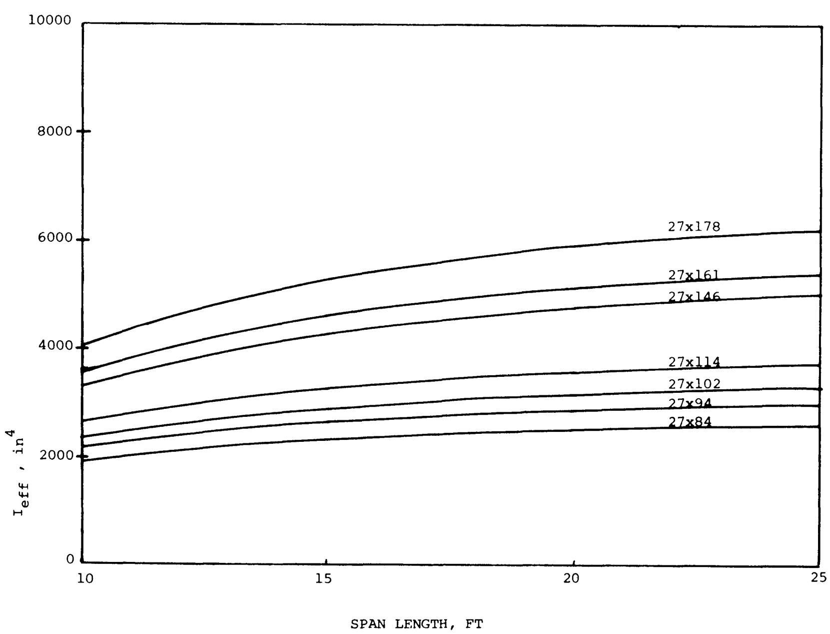

Fig. 15. Effective moment of inertia (W27)

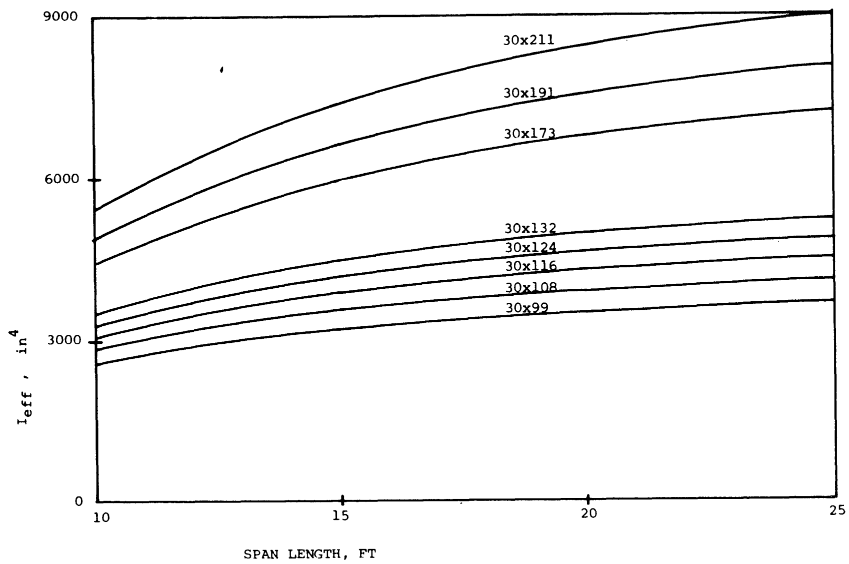

Fig. 16. Effective moment of inertia (W30)

requirements dictate the geometry of the built-up I-section, then it is a matter of proportioning between bending and shear stiffness. Defining the web ratio, R, as the ratio of the effective shear area, A' (web area), to the total cross-sectional area, A, then: $R = A'/A$

Consider a built-up section with a given cross-sectional area, depth and width. The value of I_{eff} is a linear dependent function of R, I and member length. The effect of varying web ratio, R, on the effective moment of inertia can be seen in Fig. 19. For a member length of 15 ft, with an R of 0.1, its effective moment of inertia is 14,000 in.[4] At this value, the shear leak effect is dominant. Increasing ZifR to 0.5 will increase its effective moment of inertia up to the maximum optimum value. After this value, any increase in ratio R will actually reduce its moment of inertia without increasing its effective moment of inertia. A careful ex-

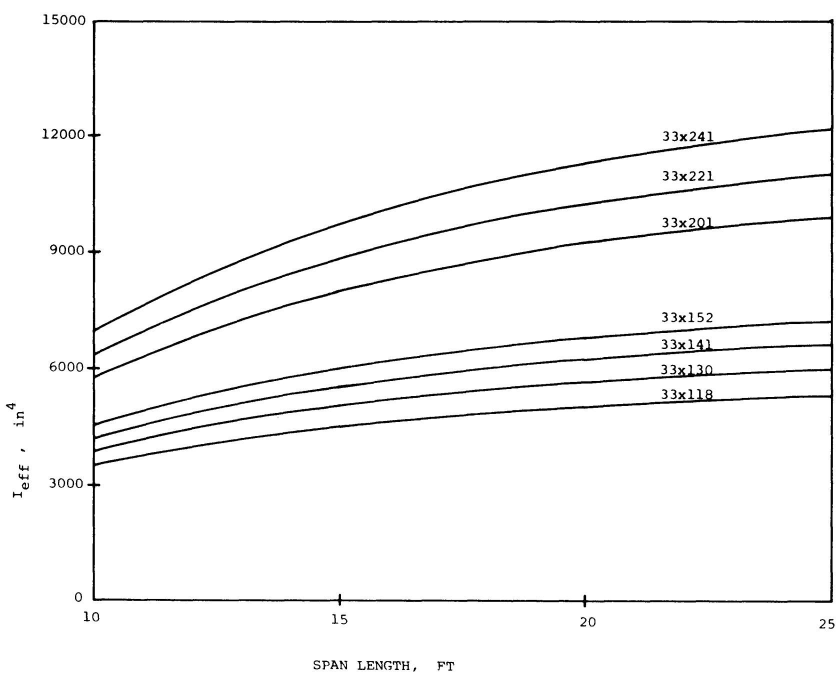

Fig. 17. Effective moment of inertia (W33)

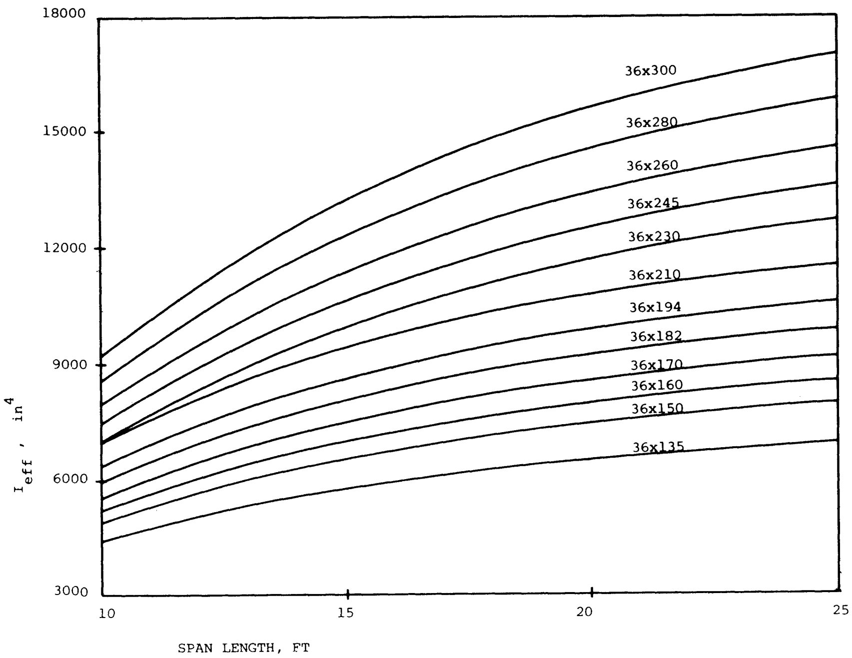

Fig. 18. Effective moment of inertia (W36)

amination of Fig. 19 further reveals that for a built-up section there is a considerable improvement in the effective moment of inertia when web ratio R is increased from 0.1 to 0.3. However, when R goes beyond 0.4 or 0.5, the variation in its effective moment of inertia is comparably smaller. In the meantime, the increase in R undercuts the moment of inertia of the section by a considerable amount, possibly to the extent that it may be critical for strength requirement. To help a designer in selecting an optimum I-section in lateral stiffness design, a series of design curves,

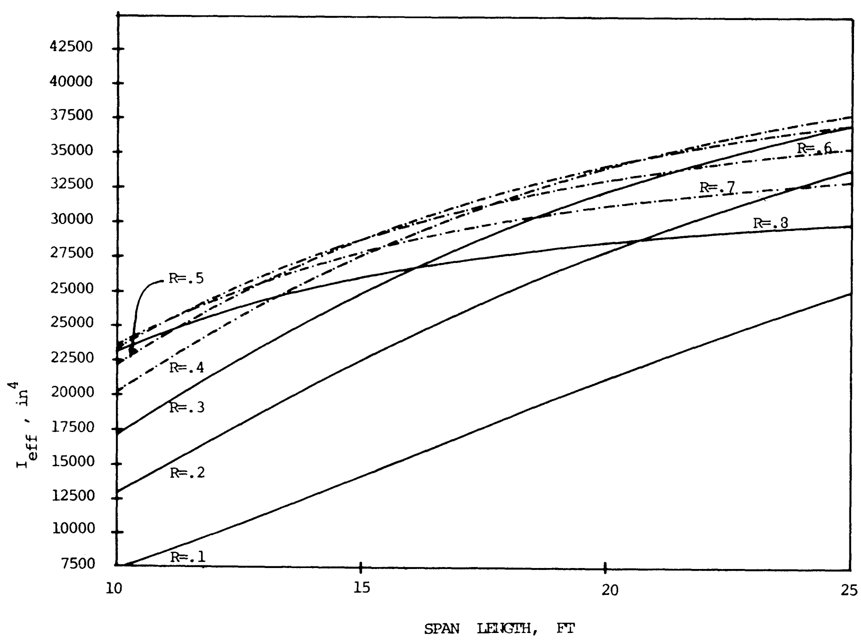

Fig. 19. Effect of varying R for constant cross-sectional area

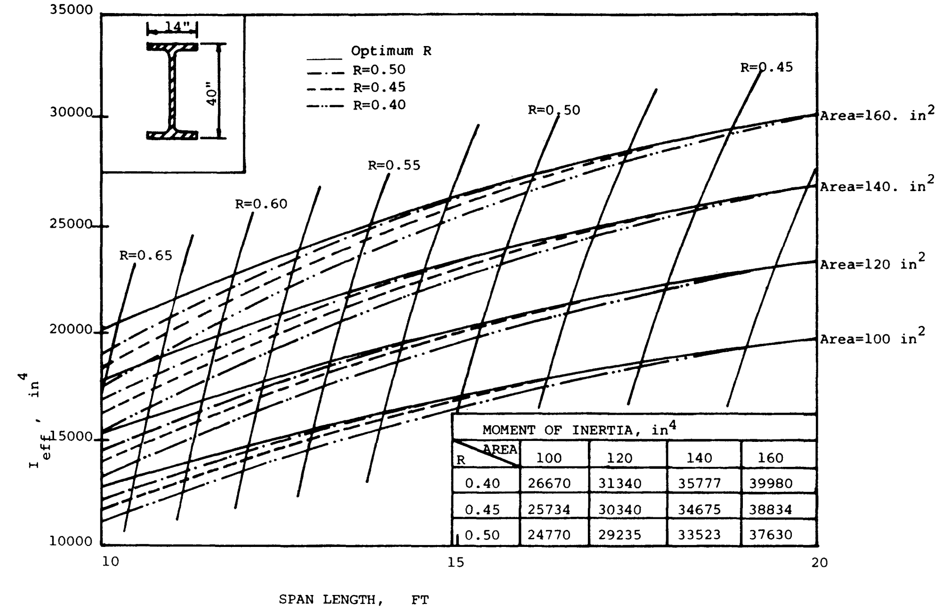

R \ AREA	100	120	140	160
0.40	26670	31340	35777	39980
0.45	25734	30340	34675	38834
0.50	24770	29235	33523	37630

Fig. 20. Effective moment of inertia (built-up section 40 x 14)

Figs. 20 through 27, is presented for the commonly used built-up sections. The sizes of the sections chosen are as follows: depth of section—40 in., 42 in., 44 in., 48 in.; width of section—14 in., 16 in.

The span lengths vary from 10 ft to 20 ft. Each figure presents the maximum I_{eff} for cross-sectional areas of 100 in.^{2}, 120 in.^{2}, 140 in.^{2} and 160 in.^{2}. The proportion of the optimum section can be interpolated from the intersecting R curves.

In order to assist a designer in selecting a member both for stiffness and strength requirements, the effective moments of inertia for web ratios of 0.4, 0.45 and 0.5 are plotted on the same set of figures for each cross-sectional area. Their moments of inertia are listed for reference.

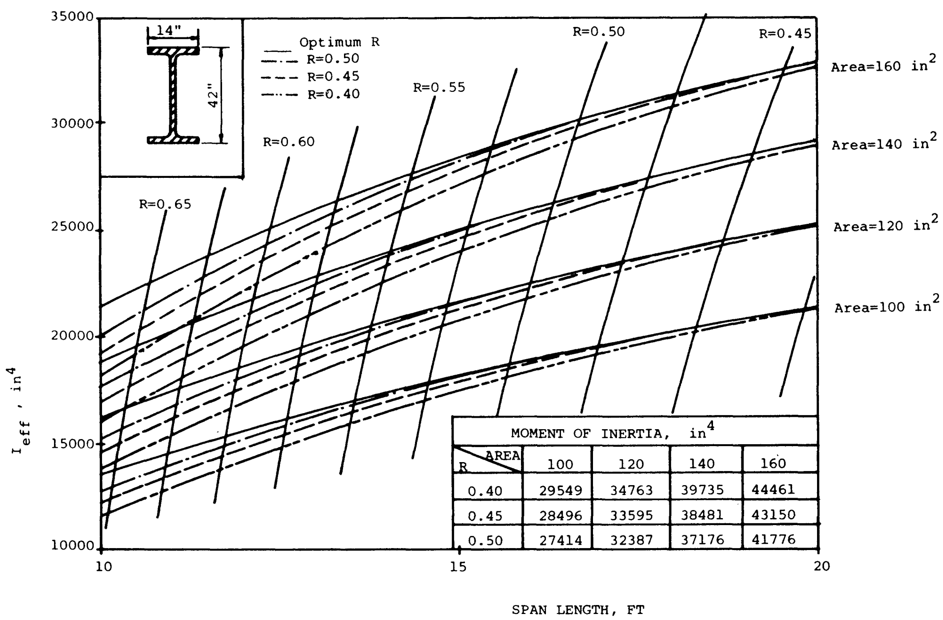

R \ AREA	100	120	140	160
0.40	29549	34763	39735	44461
0.45	28496	33595	38481	43150
0.50	27414	32387	37176	41776

Fig. 21. Effective moment of inertia (built-up section 42 x 14)

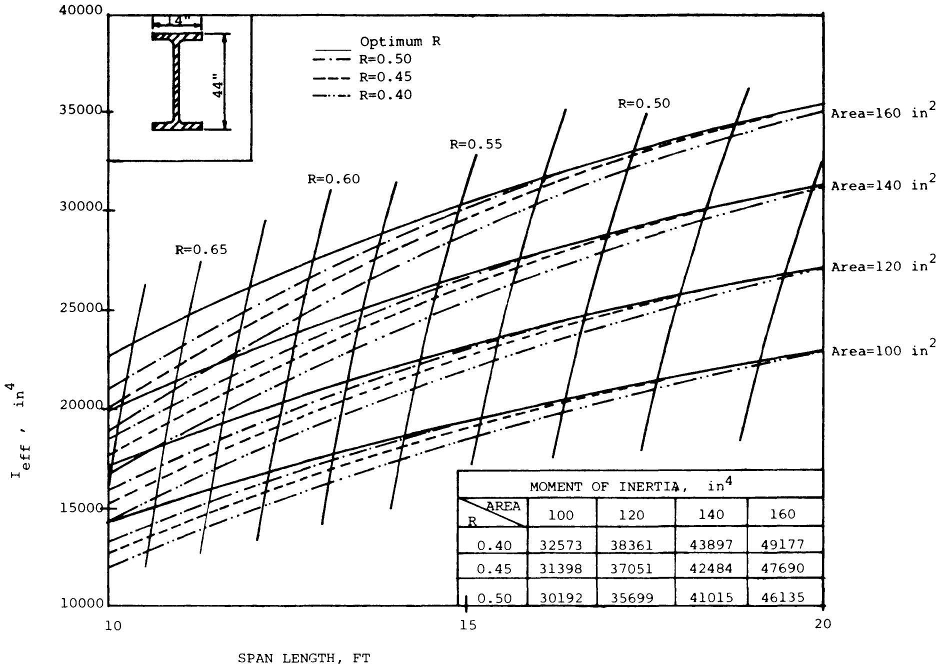

MOMENT OF INERTIA, in^4

R \ AREA	100	120	140	160
0.40	32573	38361	43897	49177
0.45	31398	37051	42484	47690
0.50	30192	35699	41015	46135

Fig. 22. Effective moment of inertia (built-up section 44 x 14)

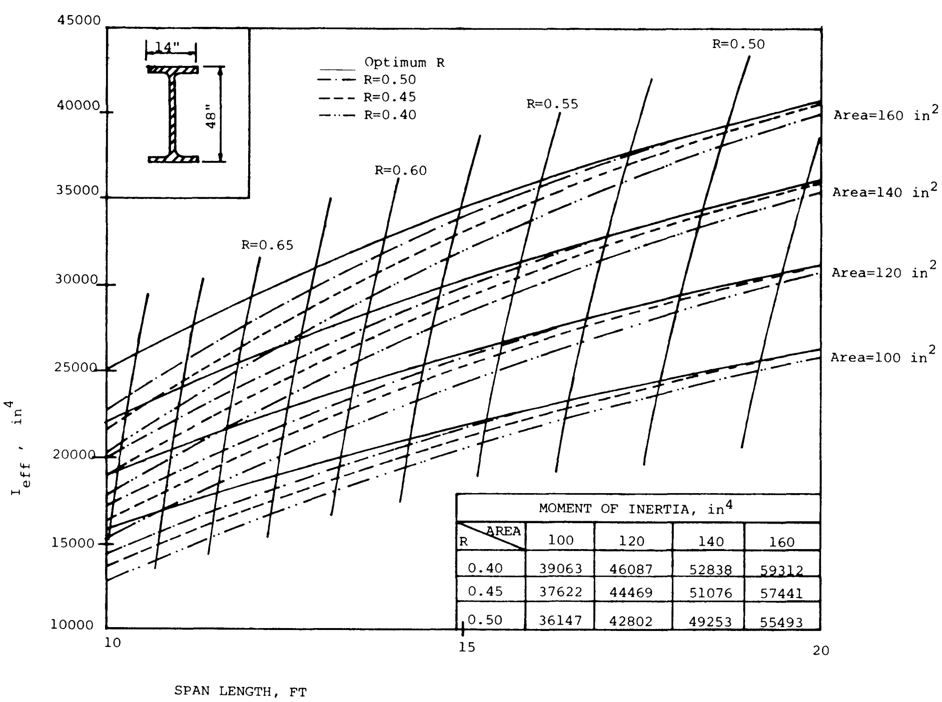

MOMENT OF INERTIA, in^4

R \ AREA	100	120	140	160
0.40	39063	46087	52838	59312
0.45	37622	44469	51076	57441
0.50	36147	42802	49253	55493

Fig. 23. Effective moment of inertia (built-up section 48 x 14)

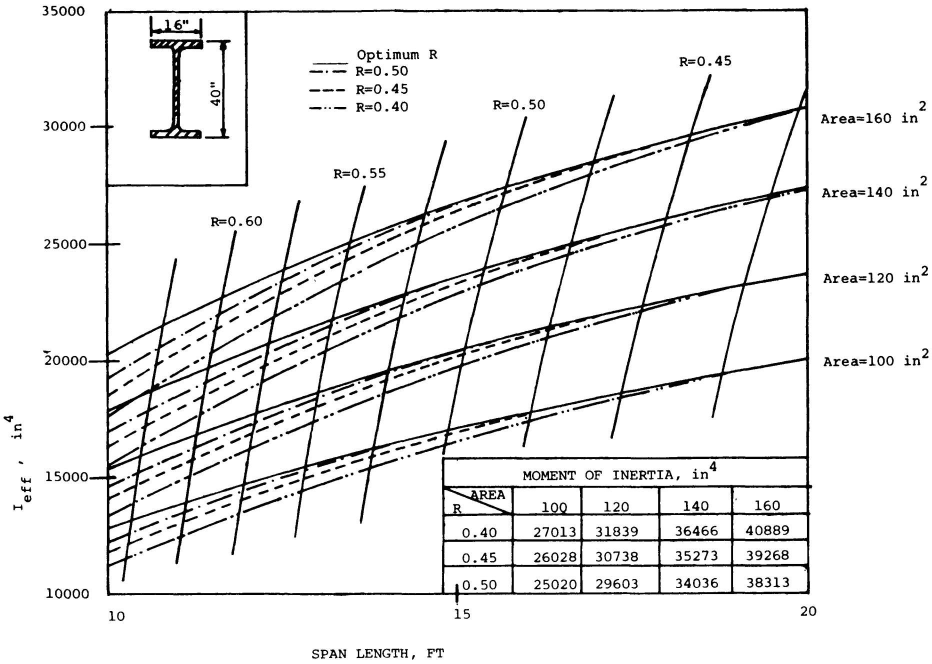

R \ AREA	MOMENT OF INERTIA, in^4 100	120	140	160
0.40	27013	31839	36466	40889
0.45	26028	30738	35273	39268
0.50	25020	29603	34036	38313

Fig. 24. Effective moment of inertia (built-up section 40 x 16)

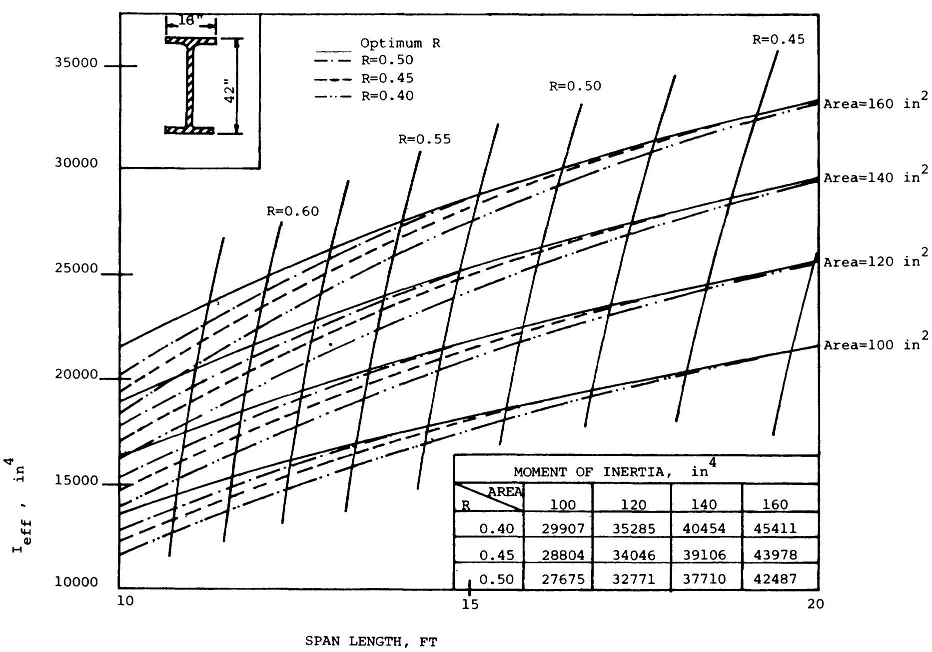

R \ AREA	MOMENT OF INERTIA, in^4 100	120	140	160
0.40	29907	35285	40454	45411
0.45	28804	34046	39106	43978
0.50	27675	32771	37710	42487

Fig. 25. Effective moment of inertia (built-up section 42 x 16)

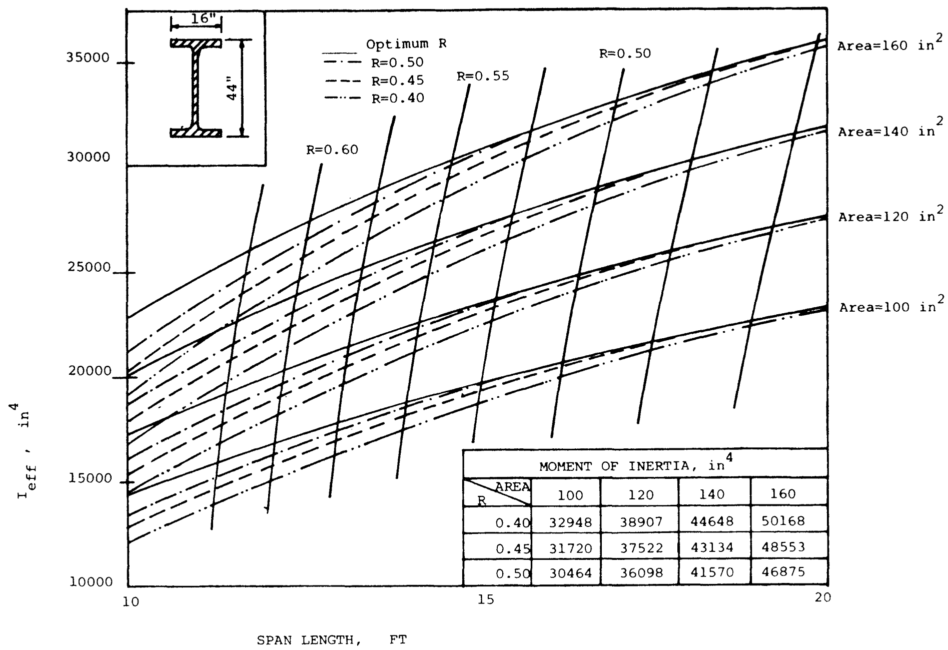

MOMENT OF INERTIA, in^4				
R \ AREA	100	120	140	160
0.40	32948	38907	44648	50168
0.45	31720	37522	43134	48553
0.50	30464	36098	41570	46875

Fig. 26. Effective moment of inertia (built-up section 44 x 16)

Use of Charts—For example, assume a designer is to select an appropriate built-up section for a beam of 15-ft span and 4-ft depth, with an effective moment of inertia of approximately 30,000 in.[4] Use the strength and stiffness charts (Figs. 20 through 27) to determine the most economical section.

Step 1.
Decide on the flange width. In this case say 14 in.; therefore, refer to Fig. 23.
Step 2.
Decide on the web ratio R. The choice is to be made from the four curves in this family of curves: $R = 0.4$, $R = 0.45$,

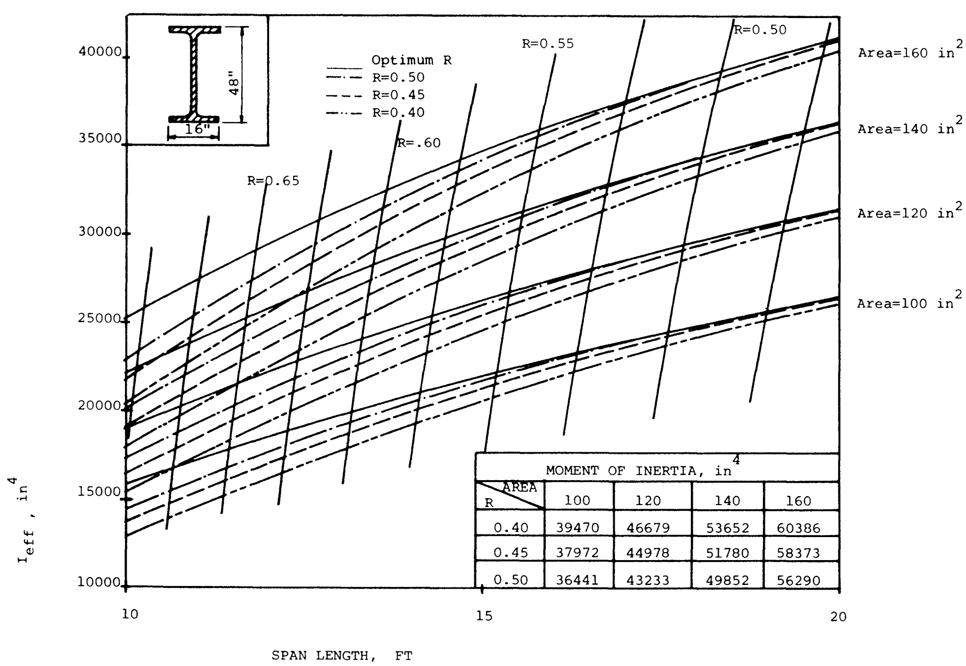

MOMENT OF INERTIA, in^4				
R \ AREA	100	120	140	160
0.40	39470	46679	53652	60386
0.45	37972	44978	51780	58373
0.50	36441	43233	49852	56290

Fig. 27. Effective moment of inertia (built-up section 48 x 16)

$R = 0.5$ and the optimum R which is indicated by the solid curve. The optimum R is associated with the section which provides the maximum effective moment of inertia for the same cross-sectional area, but usually provides the least moment of inertia.

For the optimum section:

$R = 0.574$

$I_{eff} = 34{,}300$ in.^{4}

$I = 52{,}462$ in.^{4}

For $R = 0.4$:

For $I_{eff} = 32{,}000$ in.^{4},

$I = 59{,}312$ in.^{4}

It can be seen that from a web ratio of 0.4 to the optimum web ratio of 0.574, a gain of 7% in effective moment of inertia results in a loss of 12% in moment of inertia. Hence, a designer can interpolate from the set of stiffness and strength curves to get the most economical section that will satisfy his requirements.

CONCLUSIONS

1. An efficient method for preliminary analysis and member sizing of a tall steel tubular multi-story building is developed.
2. The numerical examples demonstrated that the prediction for the deflections is excellent. The calculated bending moments and shear forces, especially at the uppermost part of the tube did not match well with the exact analysis. However, it should be noted that controlling the lateral deflection is probably the most important criterion in the preliminary stages of analysis and design.
3. The significance of shear leak deformation is demonstrated and the selection of an optimum W shape or built-up I-section is made available by the given strength and stiffness charts.
4. The proposed method of analysis is mainly applicable for rectangular shapes, but it could be extended to more general tubular shapes. Problems involving parameters like shear lag, warping, etc. are currently being studied by the authors.

REFERENCES

1. *Clough, R. W., I. P. King, and E. L. Wilson* Structural Analysis of Multi-Story Buildings *Journal of the Structural Division, ASCE, Vol. 90, No. ST3, Proc. Paper 3925, June 1964, pp. 19–34.*
2. *Fintel, M.* Response of Buildings to Lateral Forces *Report of ACI Committee 442, Title No. 68-11, ACI Journal, Feb. 1971.*
3. *Goldberg, J. E.* Wind Stresses by Slope Deflection and Converging Approximations *Transactions, ASCE, Vol. 99, 1931, p. 962.*
4. *Iyengar, S. H., N. Amin, and L. Carpenter* Computerized Design of World's Tallest Building *Computer and Structures, Vol. 2, pp. 771–783, Pergamon Press, 1972.*
5. *Iyengar, S. H.* Preliminary Design & Optimization of Steel Building Systems *Technical Committee No. 14, State of Art Report No. 3.*
6. *Khan, F. R.* Tubular Structures for Tall Buildings *Handbook of Concrete Engineering, Edited by M. Fintel, Van Nostrand Reinhold Company, 1974.*
7. *Khan, F. R. and N. R. Amin* Analysis and Design of Framed Tube Structures for Tall Concrete Buildings *Report of ACI Committee 441, Title No. 68–11, ACI Journal, Feb. 1971.*
8. *Nair, R. S.* Linear Structural Analysis of Multi-Story Buildings *Journal of Structural Division, ASCE, Vol. 101, No. ST3, Proc. Paper 11163, March 1975, pp. 551–565.*

APPENDIX A. NOMENCLATURE

A, A_o = Cross-sectional area and cross-sectional area of a cantilever, respectively
A_c , A_g = Cross-sectional area of column and girder, respectively
A' = Effective shear area
A'_c , A'_g = Effective shear area of column and girder, respectively
B = Flange width of a built-up I-section
C = Shear stiffness factor
C_c , C_g = Shear stiffness factor of column and girder, respectively
D = Depth of a built-up I-section
E = Modulus of elasticity; 29,000 ksi for steel
G = Torsional rigidity, ksi
H, H_i = Total building height and bent height, respectively
I, I_o = Moment of inertia of a section and of a cantilever, respectively
I_c , I_g = Moment of inertia of column and girder, respectively
I_{eff} = Effective moment of inertia
L_g , L_c = Span of a beam and of a column, respectively
$K_c = I_c/L_c$
$K_g = I_g/L_g$
R = Ratio of effective shear area to total area
r = Distance of a column line from center line of tube
Δ_{ci} = Lateral deflection due to cantilever action at i-th level
Δ_{bi} = Lateral deflection due to bending in frame at i-th level
Δ_{shi} = Lateral deflection due to shear in frame at i-th level
$\Delta_{fi} = \Delta_{bi} + \Delta_{shi}$
ν = Poisson's ratio = 0.25 for steel
Δ_{ti} = Total lateral deflection of floor i
V = Constant shear force